Performance of Fast FH/MFSK Signals in Jammed Binary Channels

Yu T. Su and Ruey C. Chang

***Abstract*— Soft-decision decoded performance of fast frequency-hopped (FH) M-ary FSK signals over partial band noise jammed binary channels is studied. The effects of metrics conversion, quantization, and the presence of regenerative nodes on the system's cutoff rate performance are investigated. It is found that the conversion from an M-ary metric to a binary one suffers only negligible degradations. For communication links without regenerative nodes, as expected, the infinite-bit soft-decision is the optimal metric, followed by finite-bit soft decision and then hard-decision. For those with regenerative nodes, however, the infinite-bit soft-decision is outperformed by the hard-decision, but the finite-bit soft-decision decoder still keeps its edge over the latter. The issue concerning the order of metric conversion and diversity combining is also analyzed. Numerical results indicate that the conclusion obtained by an earlier simulation report addressing a similar design alternative in fading channels is valid for jammed binary channels, as well. That is, the precombining metric conversion technique gives up only minor performance degradations when compared to the more sophisticated postcombining metric conversion technique.**

I. Introduction

The antijam (AJ) capabilities of various fast frequency-hopped (FFH) M-ary frequency-shift keying (MFSK) systems have been subjects for quite a few recent publications; see [1]–[6] and the references therein. Many of the studies concentrate on the uncoded or hard decision decoded performances for a variety of diversity combining techniques. Soft-decision decoding performance was discussed by Stark [10], Stüber *et al.* [11], [12] and Simon *et al.* [5]. In these studies, M-ary symbol codes were used in conjunction with MFSK signals; [5], [11]–[12] assumed zero thermal noise while maximum-likelihood decoding was used in [10]. The case of MFSK with M-ary codes in AWGN was analyzed by Proakis [4]. As for more practical binary codes, simulation results can be found in [16], [17]. For all these efforts, as far as we know, no analytical work on the behavior of binary coded FFH/MFSK signaling with soft-decision decoding has been reported. McGree and Deaett [16] investigated the performance of two soft-decision diversity combiners for MFSK signals over uncoded Rayleigh fading channels. The main issue they raised is the order of deinterleaving and diversity combining. The simulation results there indicated that the simpler one suffers only a modest loss (≤ 1.4 dB within the range of interest for diversity order less than six) while achieving a significant deinterleaver memory reduction. When an interleaver-deinterleaver pair is not need in the system similar design alternatives concerning the order of diversity-combining and metric conversion (see (1), (2), and Fig. 2 in the next section) still exist.

The purpose of this paper is three-fold: 1) to study the behavior of the FFH/MFSK systems with binary symbol codes and soft decision decoding against worst-case partial band noise jamming, 2) to analytically compare three soft decision alternatives (two binary and one M-ary; also see Fig. 2) for jammed/coded FFH/MFSK channels, and 3) to examine the effect of quantization and the influence of the inclusion of regenerative nodes in the above links. The ensuing section provides a description of the FFH/MFSK receiver, the system parameter definitions and the M-ary to binary metric conversion algorithm to be used. Performance analysis is presented in Section III. We first analyze the postcombining metric conversion rule using the union-Chernoff bound method developed by Omura and Levitt [7]. As will become clear later the Chernoff bound for the precombining metric conversion rule can be derived by modifying a special case of that for the postcombining metric conversion rule. The M-ary symbol case is addressed at the end of the section. Section IV deals with the effect of finite-bit quantization and regenerative nodes. Finally, numerical results, discussions, and conclusions are given in Section V.

II. System Description and Assumptions

A block diagram of the FFH/MFSK demodulator is illustrated in Fig. 2 where the outputs from various diversity branches are weighted by the reciprocals of the corresponding noise power estimations. The noise power estimation can be obtained from an AGC circuit which measures the received power in a band adjacent to the signal band, whence this receiver is sometimes called the AGC receiver [3]. We shall assume that the jammed band is much larger than an M-ary signal band so that, at any particular instant, all M potential signal channels along with the AGC channel are either jammed or unjammed simultaneously. Furthermore, we shall assume that the noise power measurement by the AGC channel is always perfect as were made in [2], [3]. In other words, the performance obtained under such a condition will be the best one can expect the AGC FH/MFSK receiver to

Paper approved by E. Biglieri, the Editor for Data Communications and Modulation of the IEEE Communications Society. Manuscript received June 5, 1991; revised August 3, 1992. This work was supported in part by National Science Council of Taiwan. This paper was presented in part at the Telecommunication Symposium, Hsinchu, Taiwan, Oct. 1990, and the IEEE International Symposium on Information Theory, Budapest, Hungary, June 1991.

Yu T. Su is with the Microelectronic and Information System Research Center and with the Department of Communication Engineering, Chiao Tung University, Hsinchu, Taiwan.

R. C. Chang was with the Department of Communication Engineering, Chiao Tung University. He is now with the Telecommunication Laboratories, Chung-Li, Taiwan.

IEEE Log Number 9401819.

achieve. There are several types of codes that can be used in conjunction with MFSK signals, for example, RS codes and dual-k convolutional codes. However, most codes used in practice are binary codes, therefore, for the purpose of binary symbol soft-decision decoding a metric conversion algorithm which converts the M-channel MFSK demodulator output into $k(\equiv \log_2 M)$ real numbers is needed. The metric (bit) conversion algorithm to be studied is [5], [10]

$$b_i = \max\{\text{metrics with the } i\text{th bit} = 1\} - \max\{\text{metrics with the } i\text{th bit} = 0\} \quad (1)$$

where $1 \leq i \leq k$.

There are some other metric conversion algorithms that had been proposed and studied [5], [13], [17] but this one was shown to be an approximate maximum likelihood (ML) metric for a general class of slowly fading channels [5, pp. 254–258]. In the case of additive white Gaussian channel similar conclusion can be reached [9, Appendix B]. For $M = 8$, the corresponding metric conversion rule is given by

$$\begin{aligned} b_1 &= \max\{a_2, a_4, a_6, a_8\} - \max\{a_l, a_3, a_5, a_7\} \\ b_2 &= \max\{a_3, a_4, a_7, a_8\} - \max\{a_1, a_2, a_5, a_6\} \\ b_3 &= \max\{a_5, a_6, a_7, a_8\} - \max\{a_l, a_2, a_3, a_4\} \end{aligned} \quad (2)$$

where $a_1, a_2, \cdots, a_8$ are the 8-ary channel outputs of the diversity combiner. Assuming, without loss of generality, that a_1 is the signal channel output and the $F_0(X)(f_0(x))$, $F_1(x)(f_1(x))$ are the probability distribution (density) functions of the noise and signal channels, respectively, then the probability density function (pdf) of b_i is given by (see Appendix)

$$P_b(x) = N[f_0(x)F_0^{N-1}(x)] \bigstar [(N-1)F_l(-x)F_0^{N-2} \cdot (-x)f_0(-x) + f_1(-x)F_0^{N-1}(-x)] \quad (3)$$

where $N = M/2$ and $\bigstar$ stands for the convolution operation. One implicit assumption in deriving (3) is that the frequency hopping pattern used by the communicator is random enough to render the channel between the encoder output and the decoder input memoryless even in the presence of jamming. As illustrated in Fig. 2 the metric conversion, which is followed by quantization in practice, can be performed either before diversity combining or after. The former requires less memory space but earlier quantizations also suffer from information loss and performance degradation. Those two design alternatives will be called as the precombining metric conversion rule and the postcombining metric conversion rule, respectively.

III. Performance Analysis

Omura and Levitt have shown [2], [7] that the decoded bit error rate (BER) for a memoryless channel can be estimated from the cut-off rate R_0 or a related parameter D which is defined by

$$D = \min_{\lambda \geq 0} D(\lambda) \quad (4)$$

$$D(\lambda) = E\{e^{\lambda[m(y,\, x';\, z) - m(y,\, x;\, z)]} | x \neq x'\}$$

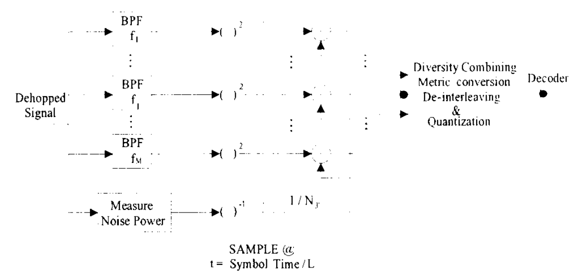

Fig. 1. Block diagram of the adaptive-gain-control (AGC) Fast FH/MFSK receiver.

where y is the decoder input, x and x' are different encoder outputs (1 or -1), z is the random variable representing side information, and $m(y,\, x;\, z)$ is the decoding metric. The relationship between R_0 and D for binary channels is well known

$$R_0 = \log_2(1 + D) \text{ bits/code symbol.} \quad (5)$$

Obviously, both D and R_0 are functions of the coding channel and decoding metric only. In contrast to the conventional cutoff rate which is defined for ML decoding metrics the cutoff defined by (4)–(5) is valid for arbitrary decoding metrics. In fact, D is the Chernoff bound for the event $\Omega \equiv \{m(y,\, x';\, z) > m(y,\, x;\, z) | x' \neq x\}$, or equivalently, $P_r\{m(y,\, x';\, z) - m(y,\, x;\, z) > 0 | x' \neq x\} \leq D \leq D(\lambda)$. Let us refer to $D(\lambda)$ as nonminimized Chernoff bound (NCB) henceforth and denote the NCB for Ω given that k out of L diversities are jammed by $D(\lambda | L,\, k)$, then these two parameters are related by

$$D(\lambda) = \sum_{k=0}^{L} \binom{L}{k} \mu^k (1-\mu)^{l-k} D(\lambda | L,\, k) \quad (6)$$

where μ is the fraction of the total hopping band jammed. With soft-decision decoding and postcombining metric conversion rule, the conditional NCB for the AGC receiver illustrated in Fig. 1 is given by (see Appendix)

$$\begin{aligned} D(\lambda | L,\, k) = &\left[\frac{M}{2} \sum_{i=0}^{M/2-1} (-1)^i \binom{M/2-1}{i} \cdot \sum_{k=0}^{i(L-1)} a_{i,k}(L)_k (1 + i - \lambda)^{-(L+k)} \right] \\ &\times \left[\frac{M/2-1}{(L-1)!} \sum_{j=0}^{M/2-2} (-1)^j \binom{M/2-2}{j} \cdot \sum_{l=0}^{j(L-1)} (-1)^{L+l+1} a_{l,j} G^{(L+l+1)}(1 + j + \lambda) \right. \\ &\left. + \sum_{m=0}^{M/2-1} (-1)^m \binom{M/2-1}{m} \cdot \sum_{n=0}^{m(L-1)} a_{n,m} (-1)^n H^{(n)}(m + \lambda) \right] \end{aligned} \quad (7)$$

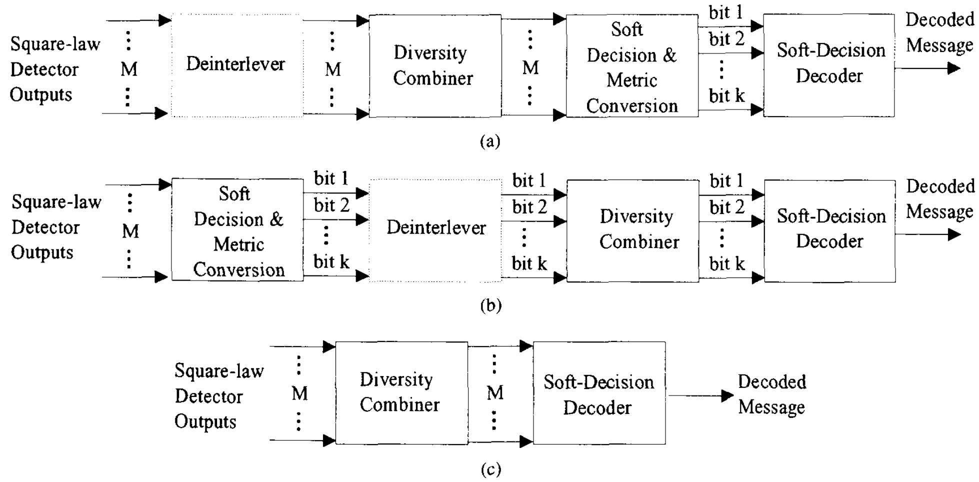

Fig. 2. Metric conversion and diversity combining for MFSK signals. (a) Postcombining metric conversion rule. (b) Precombining metric conversion rule. (c) M-ary symbol codes with soft-decision decoding.

where

$$
\begin{aligned}
0 &\le \lambda \le 1 \\
G(\lambda) &= \frac{\exp\left[-\beta_k\lambda/(1+\lambda)\right]}{[\lambda(1+\lambda)^L]} \\
H(\lambda) &= \lambda G(\lambda) \\
G^{(n)}(\lambda) &= \frac{d^n G(\lambda)}{d\lambda^n} \\
H^{(n)}(\lambda) &= \frac{d^n H(\lambda)}{d\lambda^n} \\
\beta_k &= kE_c/N_{J'} + (L-k)E_c/N_0 \\
E_c/N_{J'} &= R(\log_2 M)[E_b/(N_0 + N_J/\mu)/L] \\
E_c/N_0 &= R(\log_2 M)(E_b/N_0)/L \\
(m)_n &= \Lambda(m+n)/\Gamma(m),
\end{aligned}
$$

R is the coding rate, and $a_{i,j}$ is the coefficient of z^i in the expansion

$$\left[\sum_{m=0}^{L-1}\frac{z^m}{m!}\right]^j = \sum_{i=0}^{j(L-1)} a_{i,j} z^i. \tag{8}$$

Recursive formula for $G^{(n)}(\lambda)$ and $H^{(n)}(\lambda)$ can be found as well

$$G^{(n)}(\lambda) = \sum_0^{n-1}\binom{n-1}{i} G^{(i)}(\lambda) g^{(n-1-i)}(\lambda) \tag{9}$$

$$H^{(n)}(\lambda) = \sum_0^{n-1}\binom{n-1}{i} H^{(i)}(\lambda) h^{(n-1-i)}(\lambda) \tag{10}$$

where

$$
\begin{aligned}
g(\lambda) &= -\frac{(L+1)\lambda^2 + (L+2+\beta_k)\lambda + 1}{\lambda(1+\lambda)^2} \equiv g^{(0)}(\lambda) \\
h(\lambda) &= -\frac{L(1+\lambda)+\beta_k}{(1+\lambda)^2} \equiv h^{(0)}(\lambda) \\
g^{(m)}(\lambda) &= (-1)^{m+1} m! \\
&\quad \cdot \left[\frac{1}{\lambda^{m+1}} + \frac{L}{(1+\lambda)^{m+1}} + \frac{\beta_k(1+m)}{(1+\lambda)^{2+m}}\right] \\
h^{(m)}(\lambda) &= (-1)^{m+1} m! \left[\frac{L}{(1+\lambda)^{m+1}} + \frac{\beta_k(1+m)}{(1+\lambda)^{2+m}}\right] \\
G^{(0)}(\lambda) &\equiv G(\lambda) \\
H^{(0)}(\lambda) &\equiv H(\lambda).
\end{aligned}
$$

Note that in the above equations the dependence on β_k's have been omitted to simplify the notations. To maintain consistency we shall henceforth omit k in all related notations unless there is a danger of confusions.

As for the precombining metric conversion rule, since the statistics at different chip time and the outputs from various diversity branches are independent, we conclude that the corresponding NCB is given by

$$D(\lambda) = [(1-\mu)D(\lambda|1, N_0) + \mu D(\lambda|1, N_{J'})]^L \tag{11}$$

where $D(\lambda|1, x)$ is to be computed from (7) with $L = 1$, $k = 1$ and $\beta_1 = E_c/x$. Employing binomial expansion on the right side of (11), we find that $D(\lambda)$ for the precombining case can be obtained from that for the postcombining one by replacing $D(\lambda|L, j)$ in (6) by $D(\lambda|1, N_{J'})^j D(\lambda|1, N_0)^{L-j}$. It is also noticed that both pre- and postcombining rules yield the same performance when $M = 2$ or $L = 1$. If the same AGC FFH/MFSK demodulator is used for M-ary codes the ML decoding metric, assuming perfect side information β_k, can be shown [9, Appendix B] to be given by

$$m(n, A|k) = \ln\left[I_{L-1}(2\sqrt{\beta_k a_n})\right] - \frac{L-1}{2}\ln(a_n) \tag{12}$$

where $A = \{a_1, a_2, \cdots, a_M\}$ and a_i's are defined in (2). At high β_k the ML metric can then be approximated by

$$m(n, \lambda|\beta_k) \approx 2\sqrt{\beta_k a_n}\frac{2L-1}{4}\ln(a_n). \tag{13}$$

Hence, the metric $m(n, A|\beta_k) = a_n$ is approximately an ML one. For this metric the conditional NCB is given by

$$D(\lambda|L, k) = \frac{\exp\left[-\beta_k\lambda/(1+\lambda)\right]}{(1-\lambda^2)^L}. \tag{14}$$

Substituting (14) into (7), we then obtain the associated NCB.

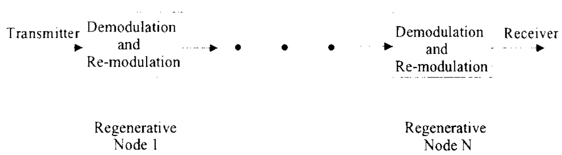

Fig. 3. A communication link with Regenerative nodes.

IV. Effects of Quantization and Regenerative Nodes

The above discussions have been restricted to direct paths with an infinite-bit precision decoding metric. In practice the decoder input is always a finite-length word, i.e., the metric converter outputs $\{b_i\}$ must be quantizied into finite-bit number before being fed into the decoder. To assess the effect of using a finite-bit quantizer we need to know the probability distribution function at the quantizer's output. Given the characteristic function for the input of the quantizer $f(\omega) = D(i\omega)$, we can utilize the inversion formula [14]

$$F(x_2) - F(x_1) = \lim_{T\to\infty} \frac{1}{2\pi}\int_{-T}^{T} \frac{e^{-itx_1} - e^{-itx_2}}{it} f(t)\, dt \quad (15)$$

and the Gil–Plaez formula [14]

$$\frac{1}{2}[F(x^+) + F(x^-)] = \frac{1}{2} \lim_{\delta\downarrow 0, T\uparrow\infty} \int_{\delta}^{T} \frac{e^{itx} f(-t) - e^{-itx} f(t)}{2\pi i t}\, dt \quad (16)$$

to obtain the output probability distribution for the N-level quantizer shown in Fig. 3:

$$\begin{aligned}\epsilon_{-N/2} &= P(-\infty < z \le \sigma_{-N/2-1}) \\ &= \frac{1}{2} - \frac{1}{\pi}\int_0^{\infty} \mathrm{Im}\,[\phi(\omega)e^{-i\omega\sigma_{-N/2-1}}]\frac{d\omega}{\omega} \quad (17)\\ &\vdots \\ \epsilon_{-1} &= P(\sigma_{-1} < z \le \sigma_0) \\ &= \frac{2}{\pi}\int_0^{\infty} \mathrm{Re}\,[\phi(\omega)e^{-i\omega(\sigma_{-1}+\sigma_0)/2}] \\ &\quad \cdot \sin[\omega(\sigma_0 - \sigma_{-1})/2]\frac{d\omega}{\omega} \quad (18)\\ \epsilon_1 &= P(\sigma_0 < z \le \sigma_1) \\ &= \frac{2}{\pi}\int_0^{\infty} \mathrm{Re}\,[\phi(\omega)e^{-i\omega(\sigma_0+\sigma_1)/2}] \\ &\quad \cdot \sin[\omega(\sigma_1 - \sigma_0)/2]\frac{d\omega}{\omega} \quad (19)\\ &\vdots \\ \epsilon_{N/2} &= P(\sigma_{N/2-1} < z < \infty) \\ &= \frac{1}{2} + \frac{1}{\pi}\int_0^{\infty} \mathrm{Im}\,[\phi(\omega)e^{-i\omega\sigma_{N/2-1}}]\frac{d\omega}{\omega}. \quad (20)\end{aligned}$$

The corresponding NCB is then given by

$$D(\lambda) = \sum_{n=1}^{N/2} [\epsilon_n e^{\lambda(2n-1)} + \epsilon_{-n} e^{-\lambda(2n-1)}] \quad (21)$$

where $N = 2^k$ for some positive integer k is assumed. For communication links with regenerative nodes (see Fig. 4) where demodulation/remodulation processes are performed, the parameter D for the end-to-end link can be obtained from that of a direct path

$$\overline{D}(\lambda) = (1-p)D(\lambda) + pD(-\lambda) \quad (22)$$

where $D(\lambda)$ is the NCB for the last segment of the link and p is the equivalent demodulated BER at the last regenerative node. Hence, if there is no decoding/re-encoding process involved in the regenerative nodes then $p = (M/2)P_s/(M-1)$, P_s = the symbol error rate. The influence of p on the overall performance can be seen by expanding the expression (22) for the N-level quantization case

$$\overline{D}(\lambda) = \sum_{n=1}^{N/2} \{[(1-p)\epsilon_n + p\epsilon_{-n}]e^{\lambda(2n-1)} + [p\epsilon_n + (1-p)\epsilon_{-n}]e^{-\lambda(2n-1)}\}. \quad (23)$$

When we compare (21) to (23), it becomes obvious that the nonzero demodulation error p has in effect redistributed the pdf $\{\epsilon_n\}$ into $\{(1-p)\epsilon_n + p\epsilon_{-n}\}$. Since $\{\epsilon_n\}$ is the pdf of a random variable representing a noise-only channel output minus the signal channel output, in general, $\epsilon_{-n} > \epsilon_n$ for $n = 1, 2, \cdots, N/2$. The resulting new pdf is thus less skewed than the original one and the overall error rate is thus increased. It can be easily found that the new pdf becomes symmetric with respect to the origin and the overall BER become 1/2 if $p = 1/2$. From the viewpoint of the decoding procedures, the influence of nonzero on the overall error rate and hence the achievable R_0 is a combined effect resulted from minimizing both terms on the right side of (22) simultaneously. Since 1) both terms are to be minimized with respect to λ and 2) $D(\lambda)$ is not a symmetric function of λ or equivalently, the probability density function of the decoder input, y in (5), is not symmetric, as is obvious from the metric conversion rule (1), the one which minimizes $D(\lambda)$ will not minimize $D(-\lambda)$ at the same time. That is, the mix-up of both correct and incorrect bits in the data stream of the final segment of the link tends to increase the number of erroneous bits contributed by individual terms, $D(\lambda)$ (correct bits being incorrectly decoded) and $D(-\lambda)$ (incorrect bits being decoded correctly) respectively. For the hard-decision (1 b quantization) case,

$$\overline{D} = \delta e^{\lambda} + (1-\delta)e^{-\lambda} \quad (24)$$

where $\delta = p + \epsilon - 2\epsilon p \approx p + \epsilon$, $\epsilon \equiv \epsilon_{-1}$, and thus $\overline{D} = 2\sqrt{\delta(1-\delta)}$.

V. Numerical Results and Discussions

Typical cutoff rate performance for the postcombining and the precombining rule with soft-decision decoding and their corresponding μ's are illustrated in Figs. 5–7. We notice that 1) increasing M does improve the performance though its effectiveness is a decreasing function of M, 2) as a result of noncoherent combining loss [19], there is an optimal diversity order for a given set of system parameters $\{M, E_s/N_0, E_s/N_J'\}$, 3) the increase of the diversity order L forces the jammer to spread his power over a wider range

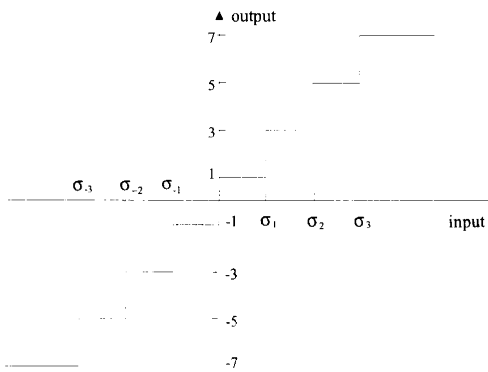

Fig. 4. An N-level quantizer ($N = 8$).

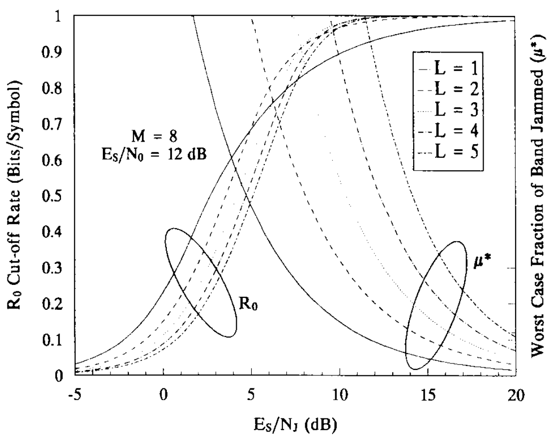

Fig. 5. Cutoff rate performance and the associated worst case μ for the post-combining soft-decision receiver; $L = 1$–5.

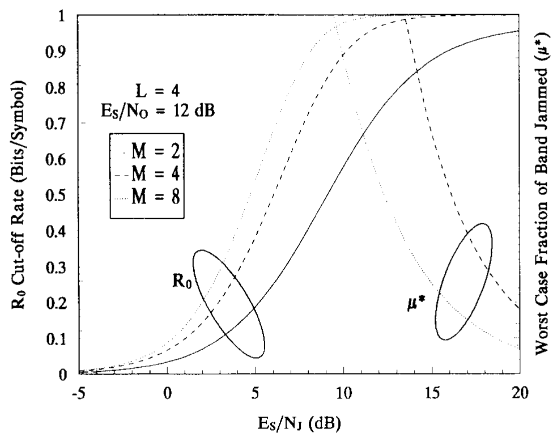

Fig. 6. Cutoff rate performance and the associated worst case μ for the post-combining soft-decision receiver; $M = 2, 4, 8$.

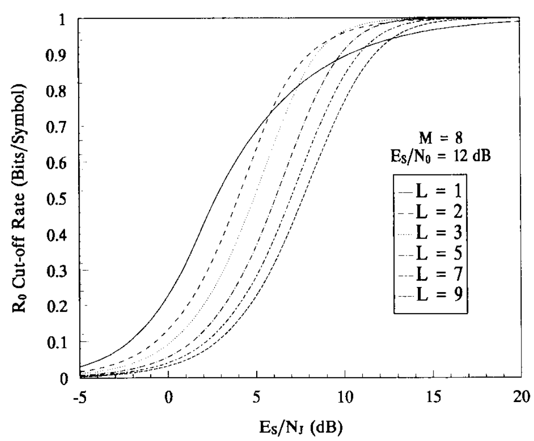

Fig. 7. Cutoff rate performance of the precombining soft-decision receiver for $L = 1$–9.

of bandwidth. On the other hand, the decrease of signal power or the increase of the jamming power enables the jammer to jam a greater portion of the signal band without compromising his jamming effectiveness. Similar observations had been obtained [1]–[3], [5]. For the convenience of comparison the performance of both receivers are put together in Figs. 8 and 9, parameterized by L and M respectively. We noted that the improvement brought about by the more complicated postcombining scheme is not significant, but it is an increasing function of both M and L. The cutoff rate performance of M-ary codes with the metric $m(A, n) = a_n$ is illustrated in Fig. 10 which exhibits a behavior similar to that of binary codes. Comparisons among various decoding metrics, including M-ary symbol codes, are summarized in Fig. 11. It can be seen that the information lost in the bit conversion process is negligible for coding rates greater than 1/2 and is less than 1 dB for most rates except when it is smaller than 0.05.

The effect of intermediate regenerative nodes are presented in Figs. 12 and 13. Obviously, the nonzero demodulation error sets a limit on the achievable R_0 for a given M, L, and E_s/N_0. The finite-bit quantization channel, however, outperforms the hard-decision and the infinite-bit precision soft-decision channels within the range of interest although the hard-decision one is as good when E_s/N_J' is high (≥ 21 dB). While for direct links the soft decision metrics outperform the hard decision one as shown in Fig. 11, the same conclusion can not be reached for indirect links any more. There is a threshold E_s/N_0 value for each L over which infinite-bit soft decoding becomes inferior to its finite-bit counterparts. Nevertheless, the finite-bit soft-decision metric still maintains its superiority over hard-decision one in this case. The reason for such a behavior can best be seen in the context of Viterbi decoding. An error event initialized by an erroneous branch metric often last several bits (or branches) before merging with the correct path again. Compared to hard-decision metric, error events generated by the second term of (22) under the soft-decision metric is more difficult to recover because of its larger "false" Euclidean distance. The finite-bit soft decision metric sets an upper limit on this kind of false increase of metric therefore avoids disastrous (large) errors and keeps its

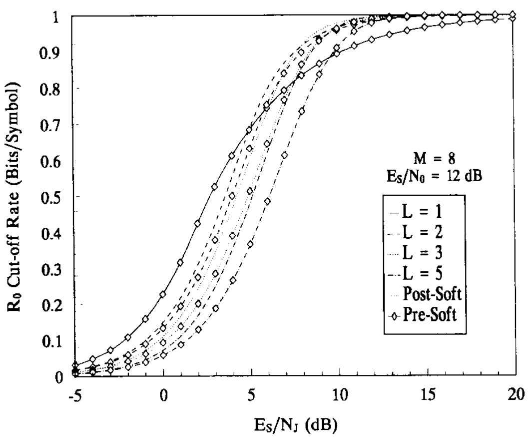

Fig. 8. Comparison of the postcombining and precombining soft-decision receivers at various diversity orders.

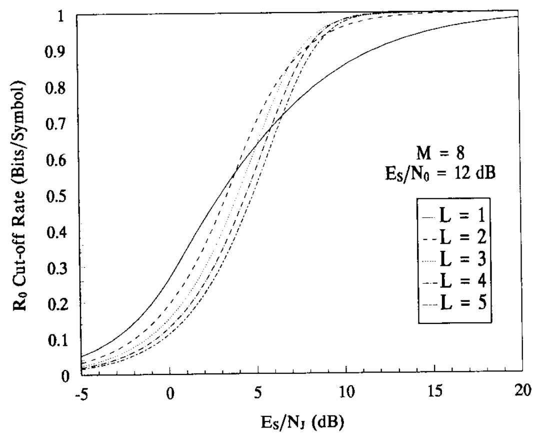

Fig. 10. Cutoff rate performance for M-ary symbol codes with soft-decision decoding.

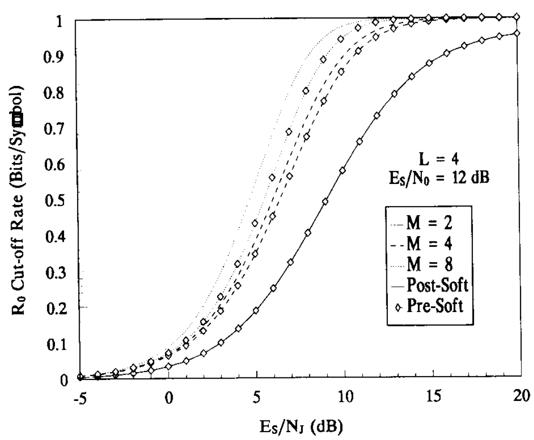

Fig. 9. Comparison of the postcombining and precombining soft-decision receivers for $M = 2$, 4, and 8.

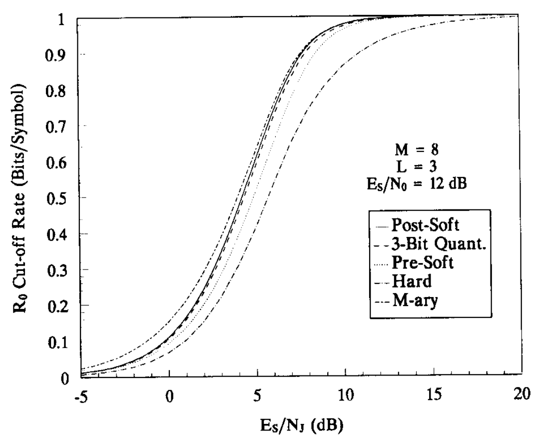

Fig. 11. Performance comparison for various receivers in a direct link.

decoding advantage. A similar argument can be applied to Euclidean (soft-decision) metric decoding of block codes.

If we assume that the cut-off rate is indeed the code rate used in the coded system then it surely makes more sense to present the performance in terms of required E_b/N_J''s [4], [10]–[12]. We depicted two such cases in Figs. 14 and 15. Although these curves look markedly different those shown before some of the relationships within a set of curves remains unchanged. If for a fixed M and E_s/N_0 the required E_s/N_J' to achieve a given R_0 at $L = L_1$ is less than that at $L = L_2$ then it is also true if we replace the E_s in the statement by E_b. However, we also notice that there is an optimum code rate for any given M and L. The optimum code rate is around 1/2 if $L = 1$ or $M = 2$ and is an increasing function of both L and M. This and other general trends shown in these figures are in fact similar to those demonstrated in [4], [10]–[12]. The broad flat portion of these curves in the R_0-axis direction is a result of noncoherent detection and AWGN channel characteristic [4, Fig. 5.2.23] though we are dealing with time-varying AWGN channel here. This portion becomes smaller if AWGN channels (time-varying or not) is replaced by Rician channels [10], and even smaller if Rayleigh channels are used instead [11]–[12].

VI. Appendix
Derivation of the Conditional NCB (7)

This Appendix is concerned with deriving (7), (9), (10) and related formulae. Without loss of generality, let us assume that channel i is transmitted. With $b_i \equiv b_{i1} - b_{i0}$ where $b_{i1} \equiv \max\{\text{metrics with the } i\text{th bit} = 1\}$ and $b_{i0} \equiv \max\{\text{metrics with the } i\text{th bit} = 0\}$, then the probability density function (pdf) for b_{i1} and b_{i0} are given by

$$\begin{aligned} f_{b_{i1}}(y) &= \frac{d}{dy} F_0^{M/2}(y) \\ &= \frac{M}{2} F_0^{M/2-1}(y) f_0(y) \qquad \text{(A.1)} \\ f_{b_{i0}}(y) &= \frac{d}{dy}[F_0^{M/2-1}(y) F_1(y)] \\ &= \left(\frac{M}{2} - 1\right) F_0^{M/2-2}(y) f_0(y) F_1(y) \\ &\quad + F_0^{M/2-1}(y) f_1(y) \qquad \text{(A.2)} \end{aligned}$$

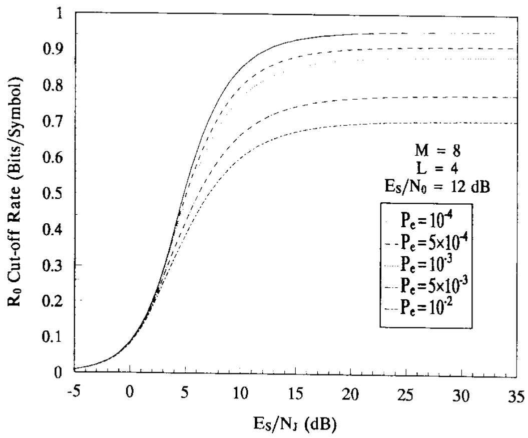

Fig. 12. Cutoff rate performance of the postcombining soft-decision decoder in various indirect links.

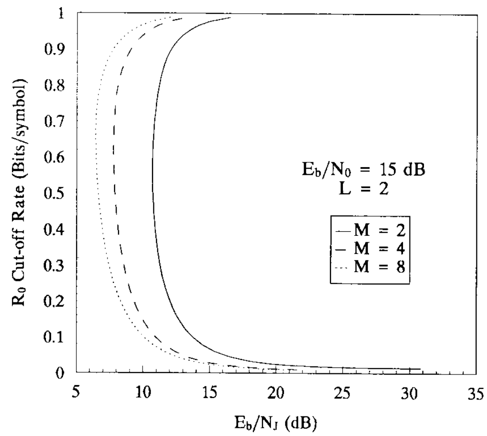

Fig. 14. Behavior of the postcombining soft-decision decoder when code rate $= R_o$, $L = 2$, $M = 2, 4, 8$.

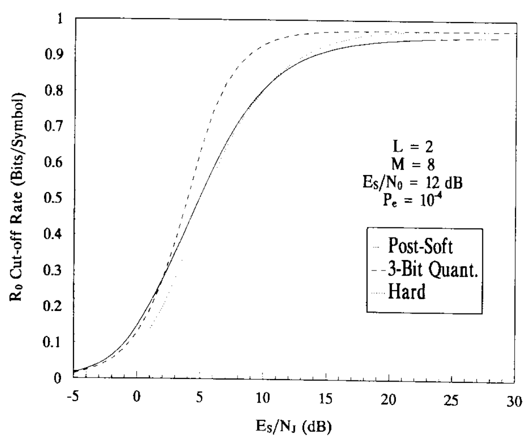

Fig. 13. The effect of intermediate regenerative nodes on different receiver designs.

where $F_0(y)(f_0(y))$ and $F_1(y)(f_1(y))$ are the probability distribution (density) functions of the diversity combiner outputs [see Fig 2(a)] for the noise and signal channels, respectively. For the PBNJ channel under consideration, $f_0(y)$ and $f_1(y)$ have the forms of

$$f_0(y) = y^{L-1}\frac{e^{-y}}{(L-1)!} \tag{A.3}$$

$$f_1(y) = \left(\frac{y}{\beta_k}\right)^{(L-1)/2} e^{y+\beta_k} I_{L-1}(2\sqrt{y\beta_k}) \tag{A.4}$$

where y is defined on positive real numbers only and L is the diversity order. The corresponding probability distribution functions are [4, ch. 1]

$$F_0(y) = 1 - e^{-y}\sum_{n=1}^{L}\frac{y^{n-1}}{(n-1)!} \tag{A.5}$$

$$F_1(y) = 1 - Q_L(\sqrt{2\beta_k}, \sqrt{2y}) \tag{A.6}$$

where $Q_L(a, b)$ is the generalized Q function defined by [4, eq. (1.1.119)]

$$Q_L(a, b) = \frac{1}{a^{L-1}}\int_b^{\infty} x^L e^{-(x^2+a^2)/2} I_{L-1}(ax)\, dx. \tag{A.7}$$

Since

$$D(\lambda|L, k) = E[e^{\lambda b_{i1}}|L, k]E[[e^{-\lambda b_{i0}}|L, k] \tag{A.8}$$

substituting (A.1)–(A.6) into (A.8) gives

$$E[e^{\lambda b_{i1}}|L, k] = \frac{M}{2}\int_0^{\infty} e^{\lambda y} F_0^{M/2-1}(y) f_0(y)\, dy \tag{A.9}$$

$$= \frac{M}{2}\int_0^{\infty} e^{\lambda y}\frac{y^{L-1}e^{-y}}{(L-1)!} \cdot \left[1 - \sum_{n=1}^{L}\frac{y^{n-1}e^{-y}}{(n-1)!}\right]^{M/2-1} dy. \tag{A.10}$$

Employing the expansion

$$\left[1 - \sum_{n=1}^{L}\frac{y^{n-1}e^{-y}}{(n-1)!}\right]^{M/2-1} = \sum_{i=0}^{M/2-1}\binom{M/2-1}{i}(-1)^i e^{-iy}\sum_{k=0}^{i(L-1)} a_{k,i}y^k \tag{A.11}$$

and substituting (A.11) into (A.10), we obtain

$$\begin{aligned} E[e^{\lambda b_{i1}}|L, k] &= \frac{M}{2(L-1)!}\int_0^{\infty}\sum_{i=0}^{M/2-1}(-1)^i\binom{M/2-1}{i} \\ &\quad \times \sum_{k=0}^{i(L-1)} a_{k,i}\int_0^{\infty} y^{L+k-1}e^{-(i+1+\lambda)y}\, dy \\ &= \frac{M}{2}\sum_{i=0}^{M/2-1}(-1)^i\binom{M/2-1}{i} \\ &\quad \cdot \sum_{k=0}^{i(L-1)} a_{k,i}(L)_k(i+1-\lambda)^{-(L+k)} \end{aligned} \tag{A.12}$$

where $(L)_k = (L+k-1)!/(L-1)!$.

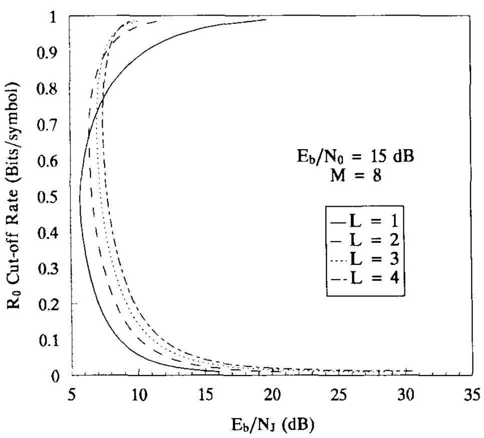

Fig. 15. Behavior of the postcombining soft-decision decoder when code rate $= R_o$, $L = 1$–4, $M = 8$.

On the other hand, the second expectation on the rhs of (A.8) can be written as

$$\begin{aligned} &E[e^{-\lambda b_{i0}}|L, k] \\ &= \left(\frac{M}{2}-1\right)\int_0^\infty e^{\lambda y}F_0^{M/2-2}(y)f_0(y)F_1(y)\,dy \\ &\quad + \int_0^\infty e^{-\lambda y}F_0^{M/2-1}(y)f_1(y)\,dy \\ &\equiv J_1 + J_2. \end{aligned} \tag{A.13}$$

The first term J_1 on the rhs of (A.13) can be expressed as

$$\begin{aligned} J_1 &= \left(\frac{M}{2}-1\right)\int_0^\infty e^{-\lambda y}F_1(y)\frac{y^{L-1}e^{-y}}{(L-1)!} \\ &\quad \cdot \left[1-\sum_{n=1}^{L}\frac{y^{n-1}e^{-y}}{(n-1)!}\right]^{M/2-2} dy \\ &= \frac{M/2-1}{(L-1)!}\sum_{i=0}^{M/2-2}(-1)^i\binom{M/2-2}{i} \\ &\quad \times \sum_{k=0}^{i(L-1)} a_{k,i}(-1)^{L+k-1}G^{(L+k-1)}(i+1+\lambda). \end{aligned} \tag{A.14}$$

While the second term on the rhs of (A.13) becomes

$$\begin{aligned} J_2 &= \int_0^\infty e^{-\lambda y}f_1(y)\left[1-\sum_{n=1}^{L}\frac{y^{n-1}e^{-y}}{(n-1)!}\right]^{M/2-1} dy \\ &= \sum_{i=0}^{M/2-1}(-1)^i\binom{M/2-1}{i} \\ &\quad \cdot \sum_{k=0}^{i(L-1)} a_{k,i}(-1)^k H^{(k)}(i+\lambda) \end{aligned} \tag{A.15}$$

where

$$G(\lambda) = \int_0^\infty F_1(y)e^{-\lambda y}\,dy = \frac{\exp\left(\frac{-\beta_k\lambda}{1+\lambda}\right)}{\lambda(1+\lambda)^L} \tag{A.16}$$

$$H(\lambda) = \int_0^\infty f_1(y)e^{-\lambda y}\,dy = \lambda G(\lambda) \tag{A.17}$$

$$G^{(n)}(\lambda) = \frac{d^nG(\lambda)}{d\lambda^n} \tag{A.18}$$

$$H^{(n)}(\lambda) = \frac{d^nH(\lambda)}{d\lambda^n}. \tag{A.19}$$

Upon substituting (A.12)–(A.15) into (A.8), we then arrive at (7) of the main text. Recursive formula for $G^{(n)}(\lambda)$ and $H^{(n)}(\lambda)$ can be derived as follows.

$$\begin{aligned} \frac{d}{d\lambda}G(\lambda) &= G(\lambda)\left[-\frac{\beta_k}{(1+\lambda)^2}-\frac{1}{\lambda}-\frac{L}{1+\lambda}\right] \\ &\equiv G(\lambda)g(\lambda). \end{aligned} \tag{A.20}$$

Consequently,

$$\begin{aligned} G^{(n)}(\lambda) &= \frac{d^{n-1}[G(\lambda)g(\lambda)]}{d\lambda^{n-1}} \\ &= \sum_0^{n-1}\binom{n-1}{i}G^{(i)}(\lambda)g^{(n-1-i)}(\lambda) \end{aligned} \tag{A.21}$$

where

$$g^{(n)}(\lambda) = \frac{d^ng(\lambda)}{d\lambda^n}. \tag{A.22}$$

Using the same procedure as that in deriving $G^{(n)}(\lambda)$, and noting that $H(\lambda) = \lambda G(\lambda)$ we arrive at

$$H^{(n)}(\lambda) = \sum_0^{n-1}\binom{n-1}{i}H^{(i)}(\lambda)h^{(n-1-i)}(\lambda) \tag{A.23}$$

where

$$h(\lambda) = -\frac{\beta_k}{(1+\lambda)^2}-\frac{L}{1+\lambda} \tag{A.24}$$

$$h^{(n)}(\lambda) = \frac{d^nh(\lambda)}{d\lambda^n}. \tag{A.25}$$

References

[1] J. S. Bird and E. B. Felstead, "Antijam performance of fast frequency-hopped M-ary NCFSK—An overview," *IEEE J. Select. Areas Commun.*, vol. SAC-4, pp. 216–233, Mar. 1986.
[2] Y. T. Su, "AJ capability of a fast FH/MFSK system in the presence of partial band noise jamming," LinCom Corp., TM-8520.05-06, IOM, Apr. 1987.
[3] J. S. Lee, L. E. Miller, and R. H. French, "Error-correcting codes and nonlinear diversity combining against worst case partial-band noise jamming of frequency-hopping MFSK systems," *IEEE Trans. Commun.*, vol. 36, pp. 471–478, Apr. 1988.
[4] J. G. Proakis, *Digital Communications.* New York: McGraw-Hill, 1989, 2nd ed.
[5] M. K. Simon *et al.*, *Spread Spectrum Communications.* Rockville, MD: Computer Science, 1985, vol. 2, ch. 2.
[6] Y. T. Su, "Fast FH/MFSK communications in band multitone jamming: Performance of a class of self-normalizing receivers," in *Conf. Rec., MILCOM'88*, Oct. 1988, pp. 44.1.1–44.1.5.
[7] J. K. Omura and B. K. Levitt, "Coded error probability evaluation for antijam communication system," *IEEE Trans. Commun.*, vol. COM-30, pp. 896–903, May 1982.
[8] M. K. Simon, "The impact of mismatch on the performance of coded narrowband FM with limiter/discriminator detection," *IEEE Trans. Commun.*, vol. COM-29, May 1981.
[9] R. C. Chang, "Performance analysis of fast frequency hopped MFSK with soft decision decoding," M.S. thesis, Nat. Chiao Tung Univ., June 1991.

[10] W. E. Stark, "Capacity and cutoff rate of noncoherent FSK with nonselective Rician fading," *IEEE Trans. Commun.*, vol. COM-33, pp. 1153–1159, Nov. 1985.

[11] G. L. Stüber, J. W. Mark, and I. F. Blake, "Diversity and coding for FH/MFSK systems with fading and jammer—Part I: Multichannel diversity," *IEEE Trans. Commun.*, vol. COM-35, pp. 1329–1340, Dec. 1987.

[12] ——, "Diversity and coding for FH/MFSK systems with fading and jammer—Part II: Selective diversity," *IEEE Trans. Commun.*, vol. 37, pp. 859–869, Aug. 1989.

[13] R. W. Boyd, "Diversity transmission of M-ary orthogonal signal in a hostile environment," in *Conf. Rec., MILCOM'83*, Oct. 1983, pp. 12–16.

[14] K. S. Gong, "Performance of diversity combining techniques for FH/MFSK in worst case partial band noise and multitone jamming," in *Conf. Rec., MILCOM'83*, Oct. 1983, pp. 17–21.

[15] B. H. Takana and R. L. Yuan, "Anti-jam performance of fast frequency hopped MFSK with coding against worst-case multitone jamming," in *Conf. Rec., MILCOM'87*, Oct. 1987, pp. 4.6.1–4.6.6.

[16] T. McGree and M. Deaett, "Pre-deinterleaving soft decision performance for MFSK detection on the Rayleigh fading channels," in *Conf. Rec., MILCOM'89*, Oct. 1989, pp. 39.2.1–39.2.7.

[17] R. A. Yost, "On the symbiotic nature of key antijamming and anti-scintillation functions for MFSK and DPSK channels," *IEEE J. Select. Areas Commun.*, vol. 5, pp. 887–894, June 1990.

[18] K. L. Chung, *A Course in Probability Theory.* New York: Academic, 1974, ch. 6.

[19] A. J. Viterbi and I. M. Jacobs, "Advances in coding and modulation for noncoherent channels affected by fading, partial band, and multiple-access interference," in *Advances in Communication Systems.* New York: Academic, 1975, vol. 4, pp. 279–308.

Yu T. Su received the B.S.E.E. degree from Tatung Institute of Technology, Taiwan, in 1974, and the M.S. and Ph.D. degrees from the University of Southern California in 1983.

From May 1983 to September 1989 he was with LinCom Corporation, Los Angeles. He is currently an Associate Professor in the Department of Communication Engineering and the Microelectronic and Information Systems Research Center at the Chiao Tung University, Taiwan. His present research interests include synchronization, equalization and antijam technologies in satellite and mobile communication systems.

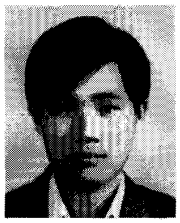

Ruey C. Chang received the B.S. degree in electrical engineering from Tatung Institute of Technology and the M.S. degree in communication engineering from Chiao Tung University, Taiwan, in 1987 and 1991, respectively.

Since July 1991 he has been with the Transmission Technology Laboratory of the Telecommunication Laboratories, Ministry of Transportation and Communications. He is currently engaged in the design of a wireless indoor communication system employing the CDMA technology.